VORTEX SHEDDING FROM A ROTATING CIRCULAR CYLINDER AT MODERATE SUB-CRITICAL REYNOLDS NUMBERS AND HIGH VELOCITY RATIO

C. Badalamenti*, S. A. Prince*
***City University, London, UK**

Keywords: *Rotating Cylinder, Vortex Shedding, Strouhal Number*

Abstract

The vortex shedding characteristics of a low aspect ratio rotating circular cylinder were investigated experimentally across a Reynolds number range (based on the cylinder diameter) of $4.1x10^4 \le Re \le 9.8x10^4$, and for cylinder-peripheral-velocity-to-freestream-velocity ratios (Ω) of $\Omega \le 4$. The results confirmed that rotation of the cylinder acted to degrade vortex shedding, and for $\Omega \approx 2$ all periodicity was apparently suppressed. At high velocity ratios ($\Omega > 3$), the unexpected re-emergence of some kind of periodicity in the wake was observed. This behaviour was believed to be associated with the formation, and migration towards the mid-span, of large trailing vortices originating at the cylinder tips. By comparison to other studies, the value of the Strouhal number (St) was found to have been affected by the low aspect ratio, high Reynolds numbers and the vibration of the cylinder, as caused by rotation. Even so, in accordance with previous experiments, the variation of Strouhal number with velocity ratio indicated a trend of increasing St with Ω.

1 Introduction

In spite of its apparent simplicity, the wake generated by a stationary circular cylinder displays a variety of highly complex phenomena. Flow separation produces a broad wake with a dominant periodicity caused by alternate vortex formation and shedding from the separated shear layers on the upper and lower surfaces. At flow velocities for which the shedding frequency is close to the natural oscillation frequency of the cylinder, the fluctuating forces arising from the shedding of vortices may cause large amplitude structural vibration or acoustic noise. Whilst studies indicate that periodic vortex shedding is at its most regular for Reynolds numbers of a few hundred (for higher *Re* the wake is complicated by the presence of turbulence), it is known that vortex shedding occurs, in one form or another, for Reynolds numbers all the way up to at least $Re = 8x10^6$ [1]. Therefore, the control of vortex shedding is of significant practical interest in many engineering applications.

Investigation has shown that steady rotation of the cylinder can be beneficial towards reducing flow-induced oscillations. However, most studies dedicated to rotating cylinders tend to concentrate on the forces generated by rotation, particularly the lift, which is known as the Magnus effect. As a result, the literature regarding the wake of a rotating circular cylinder is considerably less extensive than that pertaining to a stationary cylinder.

Due to the complexity of the flow, analytical treatments are more limited and most of the existing work is either experimental or numerical. Computational studies have largely been constrained to low Reynolds numbers ($Re \le 200$), where the wake remains laminar [2-4]. Simulations at higher *Re* [5-6] have been hampered by difficulties in obtaining converged solutions and other numerical stability problems. Furthermore, the CFD studies are almost invariably two-dimensional in nature. Experimental investigations are surprisingly few in number and have also tended to concentrate on the examination of relatively low Reynolds numbers ($Re \le 9x10^3$) [7-12].

Such previous examinations have established that the principal parameters governing the flow past a rotating cylinder are the velocity ratio, Ω (defined as the ratio of peripheral velocity at the surface of the cylinder, V_r, to freestream velocity, V), and the Reynolds number, *Re*. Of these two, the velocity ratio is the more important, being analogous to the angle of attack for an aerofoil.

Increasing the velocity ratio induces several changes in the cylinder's wake, the most important of which are found to be a progressive, asymmetric change in the position of the separation points that leads to the narrowing and biasing of the wake (towards the side where the peripheral velocity and freestream velocity are in opposition); the creation of closed streamlines about the cylinder; and the eventual suppression of the periodic nature of the wake.

Although the exact nature of the suppression process is a subject of dispute, the literature is generally in agreement that, for all Reynolds numbers for which vortex shedding from a rotating cylinder occurs ($Re \geq 47$), there is always a critical velocity ratio (Ω_c) beyond which shedding ceases. For $0 < \Omega < \Omega_c$, vortices are formed and shed alternately from the two sides of the cylinder in much the same manner as for a stationary cylinder, although an increase in the random modulation of this process is reported for $\Omega > 1$ [10, 11]. For $\Omega \geq \Omega_c$, most studies report the shedding of a single vortex from the upstream moving wall of the cylinder (where V_r and V oppose each other), with no other vortices then being shed. The value of the critical velocity ratio is known to be a function of Reynolds number, with most studies indicating that Ω_c increases with *Re* before reaching a constant value of $\Omega_c \approx 2$ when $Re \geq 200$. However, some studies indicate a higher critical ratio ($\Omega_c \approx 3$) [5].

Recent numerical simulations by Stojković *et al.* [3, 13] and Mittal & Kumar [4] suggest that, following initial suppression at Ω_c, vortex shedding from a rotating cylinder may resume for a small envelope of high velocity ratios whose boundaries are dependent on *Re*. In general, increasing the Reynolds number caused the second shedding mode to appear earlier and last longer. These investigations appear to be the first to report a resumption of vortex shedding.

Though the simulations were only performed at low Reynolds numbers ($Re \leq 200$), Stojković *et al.* [13] believed that the phenomenon should also occur at higher *Re* too. The existence of such a second region of vortex shedding at high Reynolds numbers would be of practical interest. The experimental results of Massons *et al.* [9] for $Re = 2\text{x}10^3$, $\Omega \leq 4$; Diaz *et al.* [10, 11] for $Re = 9\text{x}10^3$, $\Omega \leq 2.5$; and Tanaka & Nagano [13] for $4.5\text{x}10^4 \leq Re \leq 2.14\text{x}10^5$, $\Omega \leq 1$ do not seem to indicate any phenomena attributable to such a secondary shedding phase. Given that the onset of the second phase appears to be dependent on the Reynolds number, it may be that these tests simply did not extend to the appropriate velocity ratio at which, for the given conditions, secondary shedding would begin to occur.

The variation of the Strouhal number, *St*, with velocity ratio for $\Omega < \Omega_c$ is also a point of contention. For $\Omega \leq 1$, both experimental and numerical results show that the Strouhal number remains largely unchanged from its value when $\Omega = 0$. However, whereas the experimental data universally indicates an overall rise in *St* with velocity ratio, the numerical data are split in two: the results of some studies (all performed at $Re \geq 1\text{x}10^3$) support the experimentally observed trend [5, 6], whilst the rest (all performed at $Re \leq 200$) indicate an overall decrease in *St* with Ω [2–4]. That this discrepancy remains unexplained is due in part to the general lack of quantitative experimental data.

The existing experimental investigations of vortex shedding from a rotating cylinder have mostly been of the flow visualisation type, focusing on wake topology and the mechanisms of vortex formation and shedding. Where quantifiable data on the shedding frequency and Strouhal number has been obtained, it has typically come from experiments at low *Re* that used large aspect ratio cylinders ($AR > 10$) to promote a more two-dimensional flow. In many practical applications, conditions are likely to be less than ideal and limitations on the available space may prevent implementation of a large aspect ratio. This may then prompt the use of endplates. Furthermore, the Reynolds number of most applications will tend to be higher than the low values with which most of the literature is concerned. Understanding the influence of high Reynolds numbers, low aspect ratios and other end-effects is important as these parameters are known to significantly influence vortex shedding from stationary cylinders.

At high *Re*, the wake of a non-rotating cylinder is known to be quite disorganised and there may be competition between different modes of vortex shedding [1]. Irregularity of the wake may also be caused by a low aspect ratio. In addition, low aspect ratio stationary cylinders experience an inflow of fluid around the free ends and into the near-wake that displaces vortex formation to a region further downstream and widens the separated shear layers prior to roll up. This results in a decrease in the shedding frequency, such that the Strouhal number for a finite aspect ratio cylinder is always smaller than that for an infinite or quasi-infinite cylinder [14-16]. Although endplates may lead to an enhancement in vortex shedding uniformity, their size and shape is important. If the endplates are too small, they too may interfere with, or displace, the vortex formation region [15]. Previous research has also suggested that endplates can themselves instigate different modes of vortex shedding [17]. For low aspect ratio cylinders these effects tend to further reduce the shedding frequency.

The present work is concerned with the vortex shedding characteristics of a low aspect ratio rotating cylinder at Reynolds numbers appropriate to practical engineering application, where the flow is inherently three-dimensional and complex. Vortex shedding was examined by measuring both the time-varying and time-averaged pressures at discrete locations in the near-wake. The time-varying pressures were analysed for periodicity relating to the frequency of vortex shedding, thus enabling the Strouhal number to be assessed. Time-averaged pressures were used to provide an indication of the global spanwise wake structure and so help interpret the results. The existence at higher Reynolds numbers of a secondary regime of vortex shedding, previously noted only in low *Re* computational results, was also investigated.

2 Experimental Arrangements

Testing was carried out in City University's Handley Page laboratory using two subsonic, closed-circuit, variable speed wind tunnels (designated T2 and T3) and a cylinder of aspect ratio AR = 5.06. Pressure measurements were obtained using dynamic pressure transducers and a wake rake

2.1 Wind Tunnel Description

The T2 tunnel has a rectangular working section with 45° corner fillets and dimensions 1.12 m x 0.815 m x 1.68 m. T3 is of similar design but has a regular octagonal working section with maximum dimensions 1.15 m x 0.89 m x 1.5 m. Freestream turbulence levels in both tunnels are below 0.7% and the velocity distribution of the approach flow is known to be quite uniform, with a maximum variation of about 2% from the mean but generally varying by less than 0.5% across the majority of the working section.

Both the T2 and T3 tests were performed at freestream velocities of V = 7, 12 and 16 m/s. This provided a Reynolds number range of $4.1\times10^4 \leq Re \leq 9.8\times10^4$ (based on cylinder diameter).

2.2 The Cylinder

The cylinder was made from a hollow piece of aluminium tubing of external diameter D = 88.9 mm, length b = 450 mm and shell thickness 3.2 mm. At either end of this central tubing was an end-plug that provided support for the drive shaft. During some of the tests, the cylinder was fitted with two circular endplates having an endplate-to-cylinder diameter ratio of D_e/D = 2. The endplates were fixed to the end-plugs so that they spun with the cylinder. Each endplate was 2 mm thick and had a 45° chamfer over the outer 10 mm of the diameter. This feature reflects previous work by Apelt & West [18].

The cylinder model was suspended from the tunnel balance plate using two steel struts, which extended vertically downwards from the balance to the cylinder tips (see Fig. 1). In both T2 and T3, the cylinder was mounted horizontally, in the middle of the tunnel working section, such that its mid-span was coincident with the tunnel centerline. The ratio of cylinder diameter to tunnel height was approximately D/H = 0.11 for T2 and D/H = 0.10 for T3. This was somewhat larger than ideally desired ($D/H \leq 0.06$), but was a consequence of having to balance many conflicting constraints on cylinder sizing. Results were not corrected for wall interference due to the lack of an established procedure for the correction of rotating cylinder flow.

A Graupner Ultra 3300-7 variable speed electric motor was used to spin the cylinder. A direct-drive method was employed so as to avoid the complication of gearboxes. The motor was mounted on to the side of one of the struts supporting the cylinder, with connection between the motor and cylinder shafts accomplished via an integral-clamp-style jaw coupling. To maintain symmetry of shape, a ‘dummy motor’ was attached to the strut on the non-motor end of the cylinder (see Fig. 1). This dummy structure was made to be the same size and weight as the motor and its mounting assembly.

Power was supplied to the motor by two 12 V lead acid batteries placed in series with each other. Variation of the cylinder rpm was achieved by placing a 6.35 Ω rheostat in series with the motor. Measurement of the rotational rate was through a reflective opto-coupler positioned parallel to the endplate on the non-motor side of the support structure. Alternating black and white segments on this endplate provided a changing input to the diode when the cylinder was rotating and a custom-built interface allowed the diode’s output to be displayed on a Racal-Dana 1990 universal counter. This provided a continuous, real-time reading of the cylinder rpm. The accuracy of this optical system was tested against both a contacting mechanical tachometer and a stroboscope, with the difference between the readings from all three means being less than one percent.

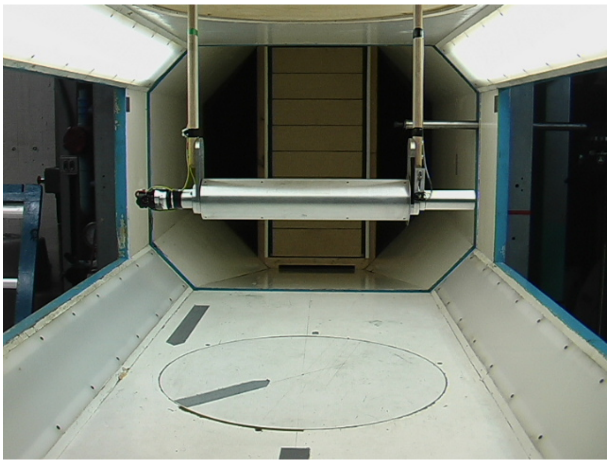

Fig. 1. Downstream view of cylinder in the T2 tunnel.

The maximum possible cylinder rotation rate before the support structure underwent unacceptable levels of vibration was found to be $N \approx 6000$ rpm. Given the range of tunnel test speeds employed, this enabled examination of velocity ratios as large as $\Omega = 4$.

2.3 Wake Pressure Measurements

Information on the wake was gathered using a wake rake and dynamic pressure transducers. The rake comprised forty pitot tubes and five static tubes. It was initially positioned vertically within the plane of the cylinder's mid-span (z/b = 0) at a downstream distance of x/D = 3, and with its centreline approximately one cylinder diameter below the cylinder's lateral axis (represented by y/D = 0, see Fig. 2). This choice ensured that the majority of the pitot tubes were located below the plane of the lateral axis and was made with the expectation, as suggested by the literature [9-11], that the wake would be deflected downwards as higher velocity ratios were implemented. Later tests moved the rake to a second downstream location, x/D = 5. In each case, pressure measurements were made at a total of twenty-four spanwise stations in the range $-0.51 \leq z/b \leq 0.45$.

Wake total pressures were recorded using a Pressure Systems, Inc. ESP-miniature pressure scanner (rated at ±2.5 psig) and a Chell

CANdaq self-contained data acquisition system. Each tube on the rake was connected to a port on the scanner. For every combination of *x/D*, *z/b*, and Ω that was to be investigated, readings from the scanner were sampled by the CANdaq system over a period of 10 s and then relayed to a PC for analysis. The resulting data were time-averaged and plotted to illustrate the spanwise structure of the whole wake and its variation with velocity ratio.

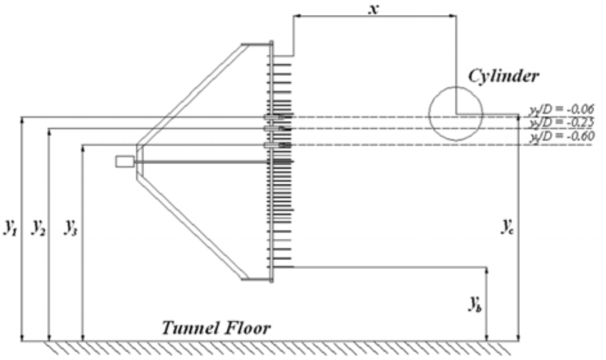

Fig. 2. Arrangement of rake and transducers relative to cylinder model.

Three Kulite CTQH-187 series dynamic pressure transducers (rated at 5 psi) were attached to the rake and similarly positioned so as to concentrate measurements on the upstream moving wall side of the cylinder. The first transducer was located as close as possible to the cylinder's lateral centreline (*y/D* = -0.06), the second, halfway to the level of the cylinder’s lower surface (*y/D* = -0.25), and the last slightly below the lower surface (at *y/D* = -0.6, see Fig. 2). The transducers were used to record analogue voltage signals that were representative of the fluctuating pressure field in the wake. These signals were digitally sampled at a rate of 300 Hz, over a period of 60 s, by using a PC running the CED Spike2 software package.

The Spike2 built-in fast Fourier transform (FFT) algorithm was used to transform the recorded pressure waveforms from the time domain to the frequency domain and so obtain the frequency power spectrum. Prior to the transform, the waveforms were digitally filtered to remove the dc offset and mains frequency (50 Hz) ac signal. The FFT was applied using a Hann window function and a block size of 512, which yielded a time resolution of 1.706 s and frequency resolution of 0.58 Hz. For each velocity ratio tested, the corresponding power spectrum was visually inspected to identify the frequency of the dominant spectral peak. With some exceptions, the most prominent peak was usually located at the shedding frequency, f_s. Once identified, this frequency was then used to calculate the Strouhal number (based on cylinder diameter).

3 Results and Discussion

The best results were obtained from tests at *Re* = $4.1\text{x}10^4$ with endplates attached and the rake (plus transducers) at *x/D* = 3. These are shown in Fig. 3. For higher *Re* it was not possible to reach velocity ratios much in excess of $\Omega = 2$ and a dominant peak at f_s was more often absent from the power spectra, making it harder to interpret the results. A similar change in the spectra occurred when testing without endplates. With increasing downstream distance, shedding activity seemed to decay quite quickly and the individual power spectra at *x/D* = 5 were both more chaotic and had smaller frequency peaks than when *x/D* = 3.

Overall, the findings were consistent with a reduction in the size of the wake and the eventual suppression of vortex shedding, as caused by high rotation. Despite the noted change in the spectra for higher *Re*, the Strouhal number results indicated that there was little difference in vortex shedding for Reynolds numbers between $4.1\text{x}10^4 \leq Re \leq 9.8\text{x}10^4$. The Strouhal number was, however, found to change slightly with both increasing *x/D* and for the cylinder without endplates, respectively increasing and decreasing in magnitude by a small amount. Even so, the same overall trend of increasing *St* with Ω was observed throughout, and, in all cases, the critical velocity ratio for suppression was $\Omega_c \approx 2$. Interestingly, at higher velocity ratios ($\Omega > 3$) there was an unexpected re-emergence of a dominant spectral peak in the results for *x/D* = 3.

Comparison with existing data shows that the present Strouhal number results seem to generally agree qualitatively, if not quantitatively, with the Diaz *et al.* [10, 11] and Tanaka & Nagano studies [12] (see Fig. 3). A particularly close match is noted at mid-level velocity ratios ($1 \leq \Omega \leq 1.5$). By contrast, the results at lower Ω (especially $\Omega = 0$) are markedly different: current results lack a region of constant Strouhal number for $\Omega \leq 1$; instead they indicate a rapid increase in *St* for all non-zero Ω. Some of these differences may be associated with the larger aspect ratio ($AR = 30$) and lower Reynolds number ($Re = 9\text{x}10^3$) of the Diaz *et al.* experiments. The lack of similarity between the present low-Ω results and the data of Tanaka & Nagano is somewhat surprising as their Reynolds number ($Re = 4.5\text{x}10^4$), downstream probe location ($x/D = 2.83$) and cylinder aspect ratio ($AR = 2.4$) all quite closely match those of the current tests. The much higher blockage ratio of the Tanaka & Nagano tests ($D/H = 0.18$) may account for the disparity.

Explanations for the trends noted in the Strouhal number results, particularly the behaviour at high Ω and the differences with other data, may be derived from a detailed examination of the form of the appropriate power spectra from which the Strouhal number was obtained (Figs. 4 and 5). This is done with reference to three flow regimes: $\Omega = 0$, $\Omega \leq 2$ and $\Omega \geq 2$.

3.1 Results with the cylinder stationary

With the cylinder stationary ($\Omega = 0$), the power spectra at all three transducer locations (see Fig. 4) revealed low-amplitude activity distributed across a broad range of frequencies ($0 \leq f \leq 40$ Hz). A single, dominant peak was somewhat difficult to identify. This situation is best illustrated in the spectrum for $y/D = -0.06$ (Fig. 4a). At this transducer location, such a low-amplitude, broadband response is not unexpected: when the cylinder is stationary, $y/D = -0.06$ lies between the two sides of the vortex street and a broadband signal can be explained by the fluid motion on the periphery of the street being diffuse [10, 11]. The lack of a dominant shedding frequency at the lower transducer locations was more surprising. Vortex shedding activity was expected to be most pronounced when the cylinder was not rotating and a large amplitude peak at the shedding frequency was anticipated, particularly for the transducer at $y/D = -0.6$ (which closely coincides with the path of the vortices shed from the lower surface).

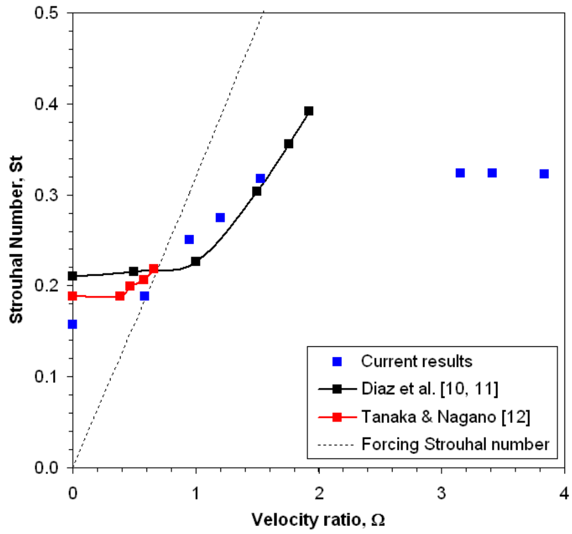

Fig. 3. Strouhal number variation with velocity ratio for $x/D = 3$, $Re = 4.1\text{x}10^4$.

Although a dominant frequency (at $f_s = 12$ Hz) was more readily identifiable for the spectra corresponding to $y/D = -0.25$ and -0.6, its amplitude remained relatively small. This was probably due to the irregularity of vortex shedding at high Reynolds numbers. The size of the dominant peak and the level of activity at other frequencies can be seen to increase with proximity to the lower extremity of the cylinder, suggesting that both are associated with vortex shedding.

Other potential origins for the activity at frequencies outside of the shedding peak were also considered. It is possible that this activity may be associated with the choice of window function applied in the FFT process; however, analysis of the original data using different functions (Hamming, Kaiser) revealed no significant changes. Pressure measurements from a test with the cylinder not in the tunnel were used to determine whether the activity was in some way associated with the freestream flow, but the shape of the power spectrum in these conditions was considerably different. These results support the notion that the observed activity was an inherent feature of the rotating cylinder wake under the test conditions.

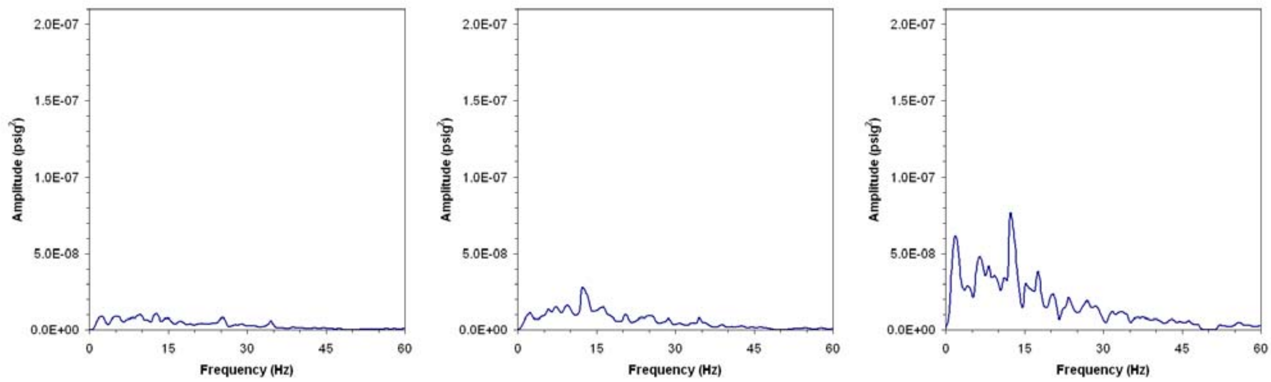

(a) y/D = -0.06 (b) y/D = -0.25 (c) y/D = -0.60

Fig. 4. Power spectra for cylinder with endplates at $Re = 4.1\text{x}10^4$, $\Omega = 0$ and $x/D = 3$.

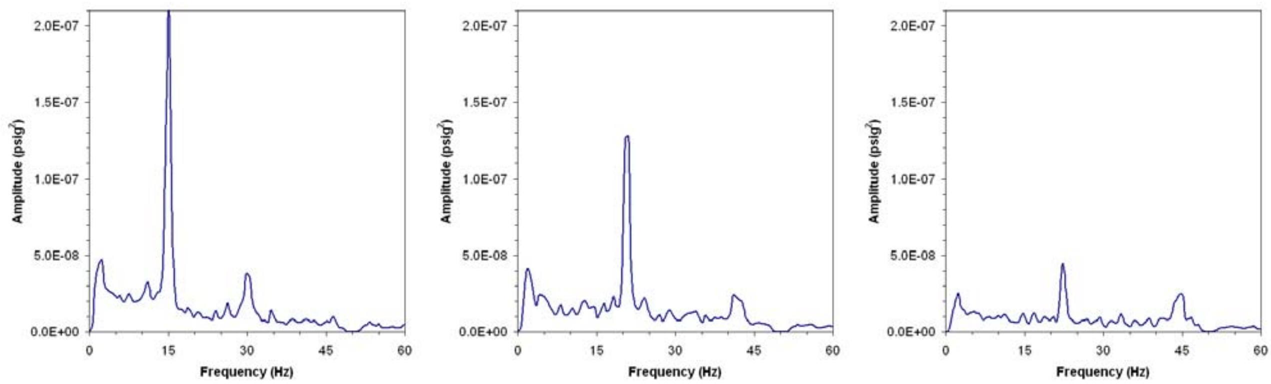

(a) $\Omega = 0.58$ (b) $\Omega = 0.95$ (c) $\Omega = 1.21$

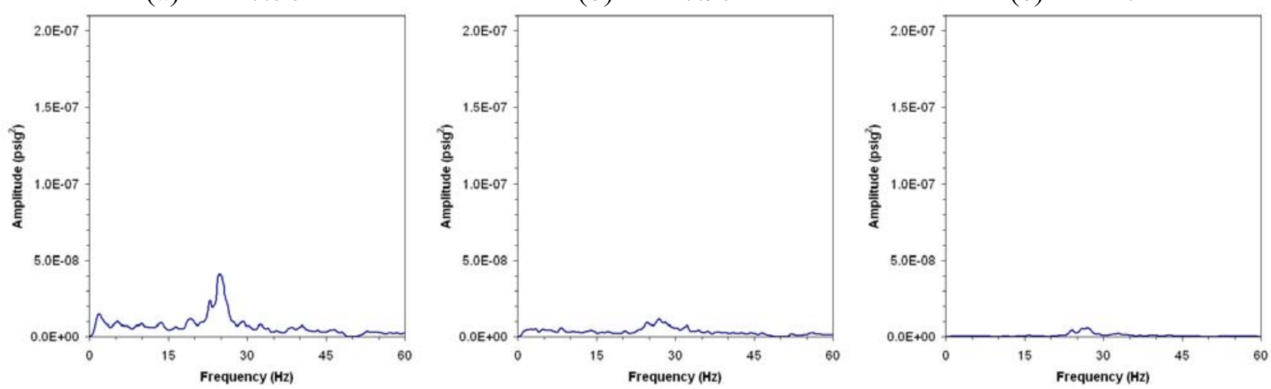

(d) $\Omega = 1.54$ (e) $\Omega = 1.88$ (f) $\Omega = 2.16$

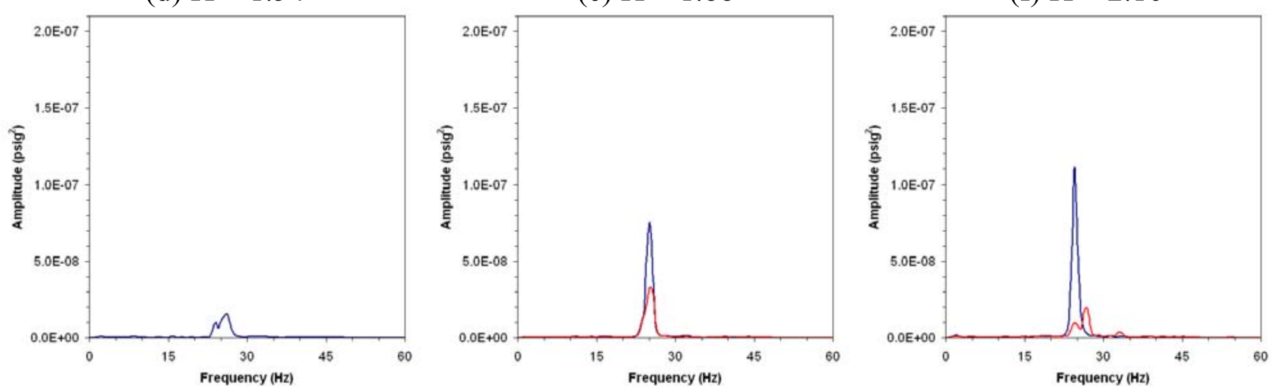

(g) $\Omega = 2.77$ (h) $\Omega = 3.14$ (i) $\Omega = 3.85$

Fig. 5. Power spectra for cylinder with endplates, measured at $x/D = 3$, $y/D = -0.6$ and $Re = 4.1\text{x}10^4$.

The Strouhal number associated with the most prominent peaks in the spectra for $\Omega = 0$ and $x/D = 3$ was found to be $St = 0.165$. The value of St obtained at $x/D = 5$ was nearly identical ($St = 0.173$). Without endplates, the Strouhal number (at $x/D = 3$) was an even lower $St = 0.13$. Such low values of St at $\Omega = 0$ are consistent with the effects of finite aspect ratio and a comparison with published data obtained under similar conditions reveals good agreement. Zdravkovich *et al.* [14] reported that the Strouhal number for a stationary cylinder of $AR = 5$ at $Re = 1.1 \times 10^5$ varied between $0.15 \le St \le 0.19$, though the irregularity caused by low aspect ratio and high Re made it impossible to assign a single value. Norberg's [16] experiments with a cylinder of $AR = 5$, having circular endplates of size $D_e/D = 10$, found the Strouhal number to be $St \approx 0.185$ at $Re = 4 \times 10^4$. This suggests that the current values are quite reasonable.

3.2 Results at low velocity ratios ($\Omega \le 2$)

With the cylinder rotating, a spectral peak associated with the vortex shedding frequency became much more prominent. This change was particularly notable in the spectra for low velocity ratios ($\Omega \le 1$, see Fig. 5a and b) and appears to indicate that rotation of the cylinder initially acted to stabilise the irregularity of vortex shedding caused by high Re and low AR. This may have been a result of rotation and vibration of the cylinder leading to 'lock-on' phenomena. Such a conclusion is supported by the fact that the Strouhal number for $\Omega \le 1$ did not remain approximately constant.

The lock-on phenomenon occurs when the forcing frequency of a body undergoing forced vibration lies in the vicinity of the shedding frequency. If the amplitude of the motion is greater than a threshold value (typically said to be 10% of the cylinder diameter, but possibly much lower [19]) it can cause a synchronizing effect wherein cylinder and wake act together and vortex shedding occurs at the vibration frequency, rather than the natural shedding frequency for the given flow conditions. This effect can alter the shedding frequency, and hence the Strouhal number, by as much as ±25% and can cause vortex shedding to be almost perfectly correlated across the span, which in turn causes the amplitude of the oscillation to increase. Such behaviour is well documented for the case of a stationary cylinder at sub-critical [20-22], critical [23] and supercritical [23] flow conditions. The lock-on effect has also previously been demonstrated for high aspect ratio rotating cylinders at very low Reynolds numbers ($Re \approx 60$) by Jaminet & Van Atta [7]; in that instance it was a result of lateral vibration and whipping of the cylinder.

In the present experiments, strong structural vibration of the cylinder occurred at rotation rates between $600 \le N \le 1600$ rpm. For the $Re = 4.1 \times 10^4$ tests, this range corresponded to $0.44 \le \Omega \le 1$. The forcing Strouhal number based on the rotational frequency of the cylinder within this range (and beyond) is plotted on the graph in Fig. 3. The closeness of this line to the Strouhal number results at $\Omega = 0.58$ and 0.95, and the level of vibration observed, indicates that the shedding frequency may have become synchronised with the rotation rate, so causing the Strouhal number to increase with it. At higher rotation rates ($2000 \le N \le 4000$), the rotational frequency and shedding frequency were no longer close enough to induce lock-on; thus, the Strouhal number returned to its true value and the results show more similarity with the data of Diaz *et al.* [10, 11].

For $\Omega > 1$, the shedding frequency peak underwent a large reduction in amplitude. This was a result of both the progressive degradation of vortex shedding activity and the biasing of the wake, which deflected the path of the vortices away from the transducer locations. The biasing and narrowing of the wake also allowed activity from both the upper and lower shed vortices to be transmitted to the transducers, resulting in the appearance of a second spectral peak (centered on the second harmonic frequency, $f = 2f_s$) that was always smaller and wider than that associated with the main shedding frequency, as seen in Figs. 5a-c.

With increasing velocity ratio the frequency spectra began to manifest changes indicative of the suppression of vortex shedding. For $1.54 \le \Omega \le 2$, the progressive reduction in the amplitude of the shedding peak was now also accompanied by a fundamental change in shape towards a broadband peak (see Figs. 5d-f). Accordingly, the Strouhal number for this region is undefined. Furthermore, the amplitude of the additional frequency peaks outside of the shedding frequency falls rapidly until they disappear completely at $\Omega \approx 2$. The disappearance of these additional frequencies at this point would seem to provide conclusive proof that they are a part of the shedding process and so vanish when it is suppressed.

That the Strouhal number showed an overall increase with velocity ratio is in keeping with the trends established by the existing experimental literature on rotating cylinders, but is in direct contrast with the majority of the CFD based studies. The existence of experimental data [7] at the same low Reynolds numbers as the CFD studies and which also shows the Strouhal number to increase with Ω suggests that the conflicting trends are not a result of differing flow conditions based on Reynolds number effects; however, the limited nature of the experimental results means such a reason cannot be completely ruled out.

Support for the experimentally observed trend may be inferred from the study of vortex shedding from stationary cylinders. The Strouhal number for an infinitely long stationary cylinder is known to increase when *Re* passes beyond the critical regime [1]. This is caused by a change in wake width. For sub-critical flow, the cylinder experiences laminar boundary layer separation and the wake width is approximately the same as the cylinder diameter. For critical and supercritical flow, the accompanying transition to turbulent separation causes the separation points to move further downstream. This reduces the wake width and forces the free shear layers to interact earlier, increasing the value of *St*. Since the effects of cylinder rotation on the separation points [5] seem equivalent to this transition-induced motion, this would appear to validate the experimental findings.

3.3 Results at high velocity ratios ($\Omega > 2$)

The spectra obtained for all three transducers at $x/D = 3$ and $2 \leq \Omega \leq 2.45$ were nearly identical in form to that obtained in a reference test in which the cylinder was absent from the tunnel while pressure measurements using the rake and transducers were made. The general form of the frequency spectrum under these conditions is illustrated in Fig. 5f. For these velocity ratios, the deflection of the wake meant that the transducer at $y/D = -0.6$ was still largely in the wake whilst those at $y/D = -0.25$ and $y/D = -0.06$ were not. Thus, the similarity across all three transducers suggests that, with the suppression of shedding, the wake flow was now indistinguishable from the freestream.

For $2.45 \leq \Omega \leq 2.77$, a small amplitude 'bump', centered on $f = 25$ Hz, appeared in the frequency spectra. When $\Omega > 2.77$, this became a sharp, distinct peak (still at $f = 25$ Hz) whose frequency remained invariant with further increases in velocity ratio, but whose amplitude grew considerably. Unlike the results at low velocity ratios ($\Omega < 1.5$), no activity was seen at any other frequency and the spectra for all three y/D locations were identical. This behaviour was seen to persist up to the limit of testing at $\Omega = 3.85$, but was found to exhibit a degree of hysteresis. The nature of the frequency peak was dependent on whether measurements had been obtained with the velocity ratio continuously increased upwards from $\Omega = 0$ (Fig. 5, blue traces) or continuously decreased downwards from $\Omega \approx 4$ (Fig. 5, red traces).

No large high-Ω spectral peaks were observed in the power spectra obtained with the rake and transducers at $x/D = 5$ and $Re = 4.1\text{x}10^4$. Instead, at this downstream location, a very small rounded peak, which was clearly distinct from the otherwise flat spectrum, was observed at $f \approx 13$ Hz when $\Omega = 2.72$. As Ω was increased, this peak became more sharply focused and slightly larger in amplitude, but then disappeared when $\Omega > 3.14$. Since this peak was much smaller and approximately half the frequency of that observed in the spectra from $x/D = 3$, it may have been a sub-harmonic.

The re-emergence of a dominant frequency peak at high velocity ratios shows some resemblance to the secondary shedding phase noted in the low *Re* computational work of Stojković *et al.* [3, 13] and Mittal & Kumar [4]. The onset of the activity at $\Omega = 3.14$ and its persistence to higher Ω is in keeping with the notion that the secondary phase appears earlier and lasts longer as Re increases. However, such similarities are only superficial and a close examination reveals considerable differences between the present findings and the nature of the secondary shedding seen in CFD studies.

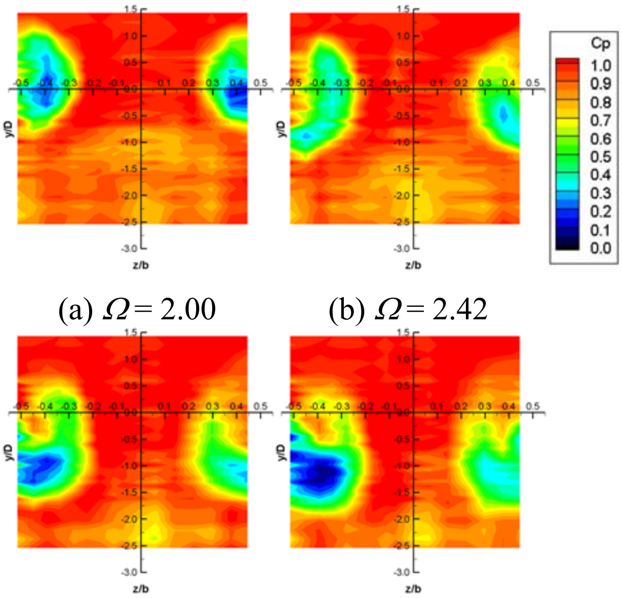

(a) $\Omega = 2.00$ (b) $\Omega = 2.42$

(c) $\Omega = 2.82$ (d) $\Omega = 3.20$

Fig. 6. Spanwise variation of time-averaged wake total pressure coefficients for cylinder with endplates at $x/D = 3$ and $Re = 4.1\text{x}10^4$.

The Strouhal number associated with this high-Ω frequency peak was the same as the last identifiable Strouhal number for the first shedding phase (St = 0.32). This is a much higher value than that reported in the CFD studies, where the Strouhal number for the second phase ($St \approx 0.05$) was found to be considerably smaller than in the first phase. Furthermore, the CFD data of Stojković *et al.* [13] show that, in the second phase, St reduces with Ω. In contrast, the present data show that, for $\Omega > 3.14$, St remained constant with increasing Ω. Most tellingly, the form of the spectra for $\Omega > 3.14$ was identical across all three transducer locations, even for those values of y/D for which the transducer would not, at these velocity ratios, be expected to be within the wake. This suggests that the spectral peak seen at $\Omega > 3.14$ was not associated with vortex shedding from the wake.

Instead, the re-emergence of a strong peak in the power spectra for x/D = 3 and $\Omega > 2.77$ seems to coincide with the evolution of a large trailing vortex system, created when the separated shear layers from the sharp edges of the cylinder or endplate tips form two counter rotating vortices, which are then swept downstream. These vortices initially began to dominate the wake at $\Omega \approx 1.5$. With increasing velocity ratio, the vortices were seen to 'roll' downwards and inwards, towards the mid-span, whilst also increasing in strength (see Fig. 6). A periodicity of the pressures near the cylinder mid-span associated with the rotation of these vortices may be responsible for the results when $\Omega > 2.77$. That the same behaviour was not observed at x/D = 5 can be explained as a consequence of the development of these vortical structures as they move downstream. At x/D = 5, the trailing vortices were found to be much stronger, but they had now rotated away from the mid-span. In this condition they may not have been able to influence the centerline, where the transducers were located, as strongly as when the rake was at x/D = 3.

4 Conclusions

The results of experimental investigation into the vortex shedding characteristics of a low aspect ratio rotating cylinder at high Reynolds number showed the same general trends as reported for more slender cylinders at lower Re, where the flow is more two-dimensional and shedding more stable. The critical velocity ratio for suppression was still found to be $\Omega_c \approx 2$ and the Strouhal number increased with increasing velocity ratio, though shedding was somewhat more irregular. Differences began to appear at higher velocity ratios, where the wake of the low AR cylinder was dominated by a large trailing vortex system and there appeared to be a return to some kind of periodicity when $\Omega > 2.7$. The apparent association with the trailing vortex system suggests that the high-Ω periodicity noted in the present results is not the same as the secondary shedding mode recently reported in some two-dimensional numerical simulations at low *Re*. That such activity has not previously been reported in other experimental studies is probably because the larger aspect ratios of most previous tests prevented the trailing vortex system from influencing the flow, whilst tests with small aspect ratio cylinders have been limited to low velocity ratios ($\Omega \leq 1$) only.

References

[1] Zdravkovich M M. *Flow around circular cylinders, volume 1: fundamentals*, Oxford University Press Inc., New York, 1997.

[2] Kang S, Choi H and Lee S. Laminar flow past a rotating cylinder. *Physics of Fluids*, Vol. 11, No. 11, pp 3312-3320, 1999.

[3] Stojković D, Breuer M and Durst F. Effect of high rotation rates on the laminar flow around a circular cylinder. *Physics of Fluids*, Vol. 14, No. 9, pp 3160-3178, 2002.

[4] Mittal S and Kumar B. Flow past a rotating cylinder. *Journal of Fluid Mechanics*, Vol. 476, pp 303-334, 2003.

[5] Chew Y T, Cheng M and Luo S C. A numerical study of flow past a rotating circular cylinder using a hybrid vortex scheme. *Journal of Fluid Mechanics*, Vol. 299, pp 35-71, 1995.

[6] Elmiligui A, Abdol-Hamid K S, Massey S J and Pao S P. Numerical study of flow past a circular cylinder using RANS, hybrid RANS/LES and PANS formulations. *22nd Applied Aerodynamics Conference and Exhibit*, Providence, RI, 2004.

[7] Jaminet J F and Van Atta C W. Experiments on vortex shedding from rotating circular cylinders. *AIAA Journal*, Vol. 7, No. 9, pp 1817-1819, 1969.

[8] Coutanceau M and Ménard C. Influence of rotation on the near-wake development behind an impulsively started circular cylinder. *Journal of Fluid Mechanics*, Vol. 158, pp 399-446, 1985.

[9] Massons J, Ruiz X and Díaz F. Image processing of the near wakes of stationary and rotating cylinders. *Journal of Fluid Mechanics*, Vol. 204, pp 167-184, 1989.

[10] Díaz F, Gavaldà J, Kawall J G, Keffer J F and Giralt F. Vortex shedding from a spinning cylinder. *Physics of Fluids*, Vol. 26, No. 12, pp 3454-3460, 1983.

[11] Díaz F, Gavaldà J, Kawall J G, Keffer J F and Giralt F. Asymmetrical wake generated by a spinning cylinder. *AIAA Journal*, Vol. 23, No. 1, pp 49-54, 1985.

[12] Tanaka H and Nagano S. Study of flow around a rotating circular cylinder. *Bulletins of the Japanese Society of Mechanical Engineers*, Vol. 16, No. 92, pp 234-243, 1973.

[13] Stojković D, Schön P, Breuer M and Durst F. On the new vortex shedding mode past a rotating circular cylinder. *Physics of Fluids*, Vol. 15, No. 5, pp 1257-1260, 2003.

[14] Zdravkovich M M, Brand V P, Mathew G and Weston A. Flow past short circular cylinders with two free ends. *Journal of Fluid Mechanics*, Vol. 203, pp 557-575, 1989.

[15] Szepessy S and Bearman P W. Aspect ratio and end plate effects on vortex shedding from a circular cylinder. *Journal of Fluid Mechanics*, Vol. 66, pp 553-576, 1974.

[16] Norberg C. An experimental investigation of the flow around a circular cylinder: influence of aspect ratio. *Journal of Fluid Mechanics*, Vol. 258, pp 287-316, 1994.

[17] Gerich D and Eckelmann H. Influence of end plates and free ends on the shedding frequency of circular cylinders. *Journal of Fluid Mechanics*, Vol. 122, pp 109-121, 1982.

[18] West G S and Apelt C J. The effects of tunnel blockage ratio and aspect ratio on the mean flow past a circular cylinder with Reynolds numbers between 10^4 and 10^5. *Journal of Fluid Mechanics*, Vol. 114, pp 361-377, 1982.

[19] Ericsson L E. Moving wall effects in unsteady flow. *Journal of Aircraft*, Vol. 25, No. 11, pp 977-990, 1988.

[20] Koopmann G H. The vortex wake of vibrating cylinders at low Reynolds numbers. *Journal of Fluid Mechanics*, Vol. 28, pp 501-512, 1967.

[21] Stansby P K. The locking-on of vortex shedding due to cross-stream vibration of circular cylinders in uniform and shear flows. *Journal of Fluid Mechanics*, Vol. 74, pp 641-665, 1976.

[22] Tokumaru P T and Dimotakis P E. Rotary oscillation control of a cylinder wake. *Journal of Fluid Mechanics*, Vol. 224, pp 77-90, 1991.

[23] Cincotta J C, Jones, Jr. G W and Walker R W. Experimental investigation of wind-induced oscillation effects on cylinders in two-dimensional flow at high Reynolds numbers. *Meeting on Ground Wind Load Problems in Relation to Launch Vehicles*, Langley Research Center, US, paper 20, 1966.

Copyright Statement